JGR Biogeosciences

RESEARCH ARTICLE
10.1029/2023JG007776

Using Relationships Between Vegetation and Surface Soil Biogeochemical Properties to Assess Regional Soil Carbon Inventories for South Baffin Island, Nunavut, Canada

Ana B. Gunther[1], Philip Camill[1], Charles E. Umbanhowar Jr.[2], Alexis Stansfield[3], and Evan N. Dethier[1,4]

[1]Environmental Studies Program and Earth and Oceanographic Science Department, Bowdoin College, Brunswick, ME, USA, [2]Departments of Biology and Environmental Studies, St. Olaf College, Northfield, MN, USA, [3]Department of Earth and Environmental Sciences, Lehigh University, Bethlehem, PA, USA, [4]Now at Department of Geology, Occidental College, Los Angeles, CA, USA

Abstract As Arctic regions warm rapidly, it is unclear whether high-latitude soil carbon (C) will decrease or increase. Predicting future dynamics of Arctic soil C stocks requires a better understanding of the quantities and controls of soil C. We explore the relationship between vegetation and surface soil C in an understudied region of the Arctic: Baffin Island, Nunavut, Canada. We combined soil C data for three vegetation types—polar desert, mesic tundra, and wet meadow—with a vegetation classification to upscale soil C stocks. Surface soil C differed significantly across vegetation types, and interactions existed between vegetation type and soil depth. Polar desert soils were consistently mineral, with relatively thin organic layers, low percent C, and high bulk density. Mesic soils exhibited an organic-rich epipedon overlying mineral soil. Wet meadows were consistently organic soil with low bulk density and high percent C. For the top 20 cm, polar desert contained the least soil C (2.17 ± 0.48 kg m^{-2}); mesic tundra had intermediate C (8.92 ± 0.74 kg m^{-2}); wet meadow stored the most C (13.07 ± 0.69 kg m^{-2}). Extrapolating to the top 30 cm, our results suggest that approximately 44 Tg C is stored in the study region with a mean landscape soil C stock of 2.75 kg m^{-2} for non-water areas. Combining vegetation mapping with local soil C stocks considerably narrows the range of estimates from other upscaling approaches (27–189 Tg) for soil C on South Baffin Island.

Plain Language Summary Warming in the High Arctic may destabilize organic carbon stored in these high-latitude soils. One challenge to estimating the amount of carbon stored in the Arctic is that data representing all major regions of the Arctic are limited. We estimate how much carbon is stored in an understudied region of the Arctic by measuring how vegetation type is related to the development of soil carbon and combining these soil data with satellite imagery to make regional estimates of soil carbon storage. On South Baffin Island, Nunavut, Canada, three major vegetation types capture the pattern of soil carbon storage. The wettest vegetation type dominated by grasses and mosses stored the most carbon, followed by a shrub-dominated vegetation type with moderate moisture. The driest vegetation type, characterized by a sparse cover of lichens and shrubs, stored the least soil carbon. Our regional estimate of soil carbon differed from other databases that predict vegetation and soil carbon. Broadly, our results suggest vegetation and hydrology are important factors for predicting how soil carbon stocks in the Arctic will change in response to climate change.

Key Points:

- Vegetation type, soil composition, and soil organic depth are important controls on soil carbon stocks in this arctic study region
- Approximately 44 Tg C is stored in the study region, differing from estimates calculated from circumpolar inventories
- Circumpolar upscaling inventories could benefit from accounting for the relationship between vegetation and soil C at fine scales

Supporting Information:

Supporting Information may be found in the online version of this article.

Correspondence to:

A. B. Gunther and P. Camill,
anagunth@umich.edu;
pcamill@bowdoin.edu

Citation:

Gunther, A. B., Camill, P., Umbanhowar, C. E., Jr., Stansfield, A., & Dethier, E. N. (2024). Using relationships between vegetation and surface soil biogeochemical properties to assess regional soil carbon inventories for South Baffin Island, Nunavut, Canada. *Journal of Geophysical Research: Biogeosciences*, *129*, e2023JG007776. https://doi.org/10.1029/2023JG007776

Received 2 SEP 2023
Accepted 15 MAY 2024

1. Introduction

Understanding the response of Arctic soil carbon (C) stocks to climate change is crucial, as these high-latitude stocks account for a significant portion of the total soil C pool (Schuur et al., 2015; Tarnocai et al., 2009). Recent efforts to constrain the Arctic soil C pool suggest that $1{,}035 \pm 150$ Pg C is stored in the top 3 m of soils in the permafrost region (Hugelius et al., 2014). The future of these stocks is challenging to predict because soil C pools may grow if arctic greening increases productivity and exceeds decomposition rates (Arndt et al., 2019; Gagnon et al., 2019; Juselius et al., 2022; Mekonnen, Riley, Berner, et al., 2021). However, soil C pools may shrink if deep soil C stocks become vulnerable to decomposition as permafrost thaws (Schuur et al., 2009; Turetsky et al., 2020). Given the size of these stocks, it is important to quantify arctic soil C pools and better understand their responses to climate change (Fisher et al., 2018).

The impact of climate change on high-arctic systems is complex because several factors control the landscape-level distribution of soil C. Prior research has shown that topographic position (Henkner et al., 2016; Weiss et al., 2017), vegetation (Bradley-Cook & Virginia, 2018; Henkner et al., 2016), and soil C (Mikola et al., 2018) are correlated in the Arctic at landscape scales. Climatic variables, including temperature and precipitation, are also important controls on soil C at local and regional scales; in general, warmer and wetter locales have higher soil C stocks (Bruhwiler et al., 2021; Mishra et al., 2021).

Topography and hydrology have shown substantial correlations with variations in vegetation composition and plant productivity in the Arctic (Campbell et al., 2021; Mekonnen, Riley, Grant, et al., 2021; Naito & Cairns, 2011). In hilly terrain, exposed peaks are often water-stressed, hill slopes are intermediate in moisture, and valleys create wet soil conditions (Mekonnen, Riley, Berner, et al., 2021). These hydrological conditions in turn influence plant structure and function, with lower plant biomass occurring on exposed topographic highs compared to slopes or valleys (Ostendorf & Reynolds, 1998; Chapin et al., 1988; R. Edwards & Treitz, 2017; Nielson et al., 2018; O'Conner et al., 2020; Mekonnen, Riley, Grant, et al., 2021). High-arctic upland areas with moderate moisture often have more shrubs and sedges, while the wet lowlands are dominated by sedges, grasses, and mosses (Campbell et al., 2021).

To the extent that interactions between vegetation and moisture control Arctic soil C stocks, improving understanding of their spatial distribution can help constrain estimates of current and future Arctic C stocks and fluxes (Henkner et al., 2016; Hobbie et al., 2000; Lamarque et al., 2023; Osono et al., 2016). Vegetation factors such as species composition, density, leaf area index, C:N ratio, and C use efficiency exert control over surface soil C stocks by altering rates of productivity and soil respiration (Atkinston & Treitz, 2012; Lamarque et al., 2023; Mekonnen, Riley, Grant, et al., 2021). However, disagreement remains on which vegetation types store more C: several studies suggest that graminoid and wetland vegetation types store the most soil C in the Arctic (Bradley-Cook & Virginia, 2018; Horwath Burnham & Sletten, 2010; Palmtag et al., 2015; Petrenko et al., 2016), but other studies have indicated that shrub tundras store more C (Elberling et al., 2004; Gries et al., 2020). In addition to vegetation, soil moisture also affects the vertical distribution of arctic soil C stocks (Gries et al., 2020; Mishra & Riley, 2012; Natali et al., 2015). Highly saturated soils are associated with deeper organic horizons because microorganisms are less efficient in low-oxygen conditions, thereby slowing decomposition (Broll et al., 1999). In arctic environments, higher soil moisture may also increase cryoturbation, which buries surface organic C and increases C storage (Gries et al., 2020; Gundelwein et al., 2007; Harden et al., 2012; Palmtag et al., 2015).

Several approaches have been developed to quantify the relationship between landscape characteristics and soil C and to scale up local soil C storage estimates to regional and pan-arctic scales (Atkinston & Treitz, 2012; Hugelius, 2012). At local and regional scales, high-resolution remote sensing approaches using both topography and land cover classification are an increasingly common method for upscaling soil C stock assessments (Hugelius et al., 2011; Palmtag et al., 2015, 2018; Siewert et al., 2016; Weiss et al., 2017; Wojcik et al., 2019). Applying a land cover-based upscaling to the pan-arctic scale may be possible with the recently published 1-km raster version of the Circumpolar Arctic Vegetation Map (CAVM), although the resolution may still be too coarse to represent highly variable arctic environments (CAVM Team, 2022). At the pan-arctic scale, three different methods of estimating soil C stocks exist: the Northern Circumpolar Soil Carbon Database (NCSCSD) (Hugelius et al., 2014), the SoilGrids database (Poggio et al., 2021), and the C-Band SAR approach (Bartsch et al., 2016). The NCSCD is a thematic upscaling that links 1,778 soil pedons with soil C data to upscale soil C stocks for the circumpolar permafrost region of the Arctic (Hugelius et al., 2014; Tarnocai et al., 2009). SoilGrids is a global database that uses soil profiles combined with environmental covariates like vegetation and hydrology to predict soil C at 250-m resolution (Batjes et al., 2020; Poggio et al., 2021). Finally, C-Band SAR is used to measure and upscale soil C by remotely sensing surface roughness and vegetation structure as a proxy for soil C content (Bartsch et al., 2016; Yonghong et al., 2023).

At least three limitations hinder efforts to scale local measurements of soil C to regional and pan-Arctic assessments of soil C stocks. First, the current spatial distribution of high-arctic soil sampling is limited and does not represent the heterogeneity of arctic regions/landscapes (Lara et al., 2020; Metcalfe et al., 2018; Virkkala et al., 2019). Several regions, including the Canadian high-arctic archipelago, are underrepresented compared to other regions, such as Alaska and Western Russia, which have been studied more thoroughly (Hugelius et al., 2014). Second, additional measurements of soil C are needed to characterize how C stocks change with major arctic vegetation types and soil depth. This is particularly the case for high-arctic wetland systems, which

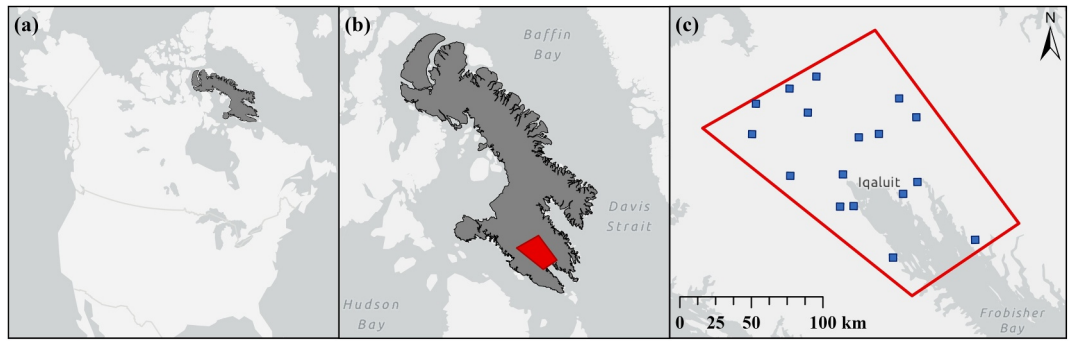

Figure 1. (a) The geographic location of Baffin Island (gray shaded) in Canada, (b) location of the study region on southern Baffin Island (red box), and (c) location of the 17 sampling sites in this study (blue squares) relative to the location of the city of Iqaluit, Nunavut.

have been incompletely studied, yet may be the most responsive to vegetation greening and soil C pool growth (Bakian-Dogaheh et al., 2022; Nabe-Nielson et al., 2017; O'Conner et al., 2020). Third, efforts to scale up local soil C measurements to regional and pan-arctic-scale stock assessments can benefit from the application of high-resolution, remote-sensing-based land cover classifications. Limitations exist for each of the methods used to estimate pan-arctic soil C. The NCSCD, CAVM, and C-Band SAR may be too low resolution to accurately assess variability in high-arctic soil C stocks, while both SoilGrids and the NCSCD database are limited by the lack of soil C data from different geographies (Bartsch et al., 2016; Mishra et al., 2013, 2021; Poggio et al., 2021; Weiss et al., 2017).

We present new soil C measurements and a high-resolution vegetation classification from South Baffin Island, Nunavut, Canada, and use these to improve estimates of regional soil C stocks in this region. Baffin Island is an arctic region poised to green significantly because of its combination of moderate warmth but wetter conditions than other regions in the Canadian Arctic Archipelago (Maxwell, 1981). It is also an understudied region of the Arctic (Virkkala et al., 2019), with few field studies of soil C (Bockheim, 1979; Broll et al., 1999; Evans & Cameron, 1979) and no published estimates of soil C stocks. Using a combination of soil cores and high-resolution imagery, we address the following specific questions: (a) How do organic depth, bulk density, percent C, total soil C, and soil C:N vary across major high-arctic vegetation types (polar desert, mesic tundra, wet meadow) and with soil depth? (b) How well does high-resolution satellite imagery classify these major vegetation types in this region? (c) How do upscaled estimates of soil C stocks in this region using these field measurements of soil C and high-resolution vegetation mapping compare to previous soil C stock estimates (NCSCD, SoilGrids, C-Band SAR) or upscaling estimates generated from lower-resolution vegetation mapping (CAVM)?

2. Materials and Methods

2.1. Study Region

The study region is located within a 100-km radius of the capital city of Iqaluit (63.75°N, 68.52°W) on South Baffin Island, Nunavut, Canada (Figure 1). As the largest island in the Canadian Arctic Archipelago, Baffin Island is approximately 1,500 km in length and parallels Greenland (Corbett et al., 2016). South Baffin Island is categorized as Low Arctic, although it is located near the transition between the Low Arctic and the High Arctic (Prowse et al., 2009). The study region is within bioclimate Subzone D, where rates of greening are correlated with summer warmth (Jia et al., 2009). For the period 1981–2010, mean annual temperature in Iqaluit was −9.8°C, and mean annual precipitation was 412 mm (Environment Climate Change Canada, 2023). The region has experienced a 1.6°C increase in temperature (Ford et al., 2017) and a more than 20% increase in precipitation (Mekis & Vincent, 2011) over the past 70 years.

South Baffin Island lies north of the tree line, and the vegetation is dominated by herbs, shrubs, and lichens (Prowse et al., 2009). CAVM estimates that the study region has a high coverage of bedrock (B2), with the vegetated areas including prostrate dwarf-shrub tundras (P1, P2) and moist sedge and dwarf tundras (G3) (CAVM Team, 2022). Non-bedrock areas have been estimated to have 80%–100% vegetation cover (Gould et al., 2003). Aboveground biomass ranges from 500 to 2,000 g m^{-2}, which is slightly higher than other regions of Subzone D

(100–2,000 g m^{-2}) (Gould et al., 2003). Previous work has shown that vegetation types on South Baffin Island are correlated with topography and moisture (R. Edwards & Treitz, 2017).

The study area lies within the continuous permafrost zone (Prowse et al., 2009) and its soils are predominantly classified as Gelisols (Aide et al., 2021). Within the Gelisol class, Turbels and Orthels are present in the study region (Tarnocai et al., 2009). These soils are acidic, with a high proportion of gravel and sand and low clay content (Evans & Cameron, 1979). In previous research, Baffin soils have been described as highly variable due to differences in vegetation and microclimate (Bockheim, 1979). Organic matter content is higher in soils developed from dwarf shrub, sedge, and moss tundras. Polar deserts support lower organic content and are located on high altitudes and crests with sparse lichen covers (Bockheim, 1979). Moist soils often have higher C content than dry soils because cryoturbation transports organic C to lower depths, where it is too cold to be decomposed (Broll et al., 1999).

2.2. Field Sampling

In July 2022, we collected a total of 51 soil cores from 17 sites that spanned a range of major vegetation types, topographic positions, and hydrological conditions in the region (Figure 1c). The locations of the 17 sites were chosen to ensure that sampling locations were spatially independent. We adopted the vegetation/land cover classification system of R. Edwards and Treitz (2017), which was developed in the Apex River Watershed within the study region and characterized landscapes using four major categories (from decreasing to increasing moisture): (a) barren, (b) polar desert, (c) mesic tundra, (d) wet meadow tundra. These land cover types were chosen because the three vegetation types—polar desert, mesic tundra, and wet meadow—are correlated with topographic position and hydrological gradients (Figure 2, Table 1). These correlations with vegetation type were assessed qualitatively in the field and described by R. Edwards and Treitz (2017). To assist with locating wet meadow tundra ecosystems, we identified potential study sites using remote sensing to find areas of high NDVI within the sedge, dwarf-shrub, and moss tundra (G3) polygons from CAVM (CAVM Team, 2003; Walker et al., 2005). Polar desert and mesic tundra vegetation types were sampled in the surrounding uplands at each site. Areas classified as barren were not sampled because they often consisted of exposed bedrock with no soil development.

At each of the 17 sites, we collected three soil cores, one from each vegetation type. Because of the nature of the vegetation and soil structure (Figure 3), we developed different sampling approaches for each vegetation type. For polar desert soils, we excavated a trench to ∼20 cm depth and sampled the 0–10 cm and 10–20 cm intervals along one of the exposed faces using a 5.27-cm-diameter steel cylinder driven vertically into the soil with a sledgehammer (Figure 3a). For the mesic tundra cores, we collected the top (living/organic) portion of the soil separately from the mineral soil. A trench was excavated to ∼20 cm depth, and the depth of the organic-mineral transition was noted (Figure 3b). A ∼5-cm (width) x ∼5-cm (length) monolith of the organic portion was excavated from one of the exposed faces to the depth of the transition between organic and mineral soil (mean depth = 6.9 cm, $n = 17$). The soil cylinder was used to collect mineral soil to a depth of 10 cm and, additionally, from 10 to 20 cm. Because the wet meadow sites were dominated by *Sphagnum* peatmosses, we used techniques described previously for sampling peat in permafrost soils (Camill et al., 2017). We first extracted a peat monolith with a bread knife to the depth of permafrost, when present, or to the depth of rock or mineral soil (Figure 3c). When permafrost was detected at depths shallower than the depth of peat, a Hoffer corer was used to extract frozen soil to a depth of rock or mineral soil (Camill et al., 2017; Zoltai, 1978). Soil sampling was limited to the top 20 cm in the polar desert and mesic tundra vegetation types due to the difficulty of sampling upland soils containing stones and permafrost. In the wet meadow sites, accumulations of stone-free peat permitted sampling to the depth of rock/mineral soil (mean depth = 40.1 cm, range = 10–151 cm, $n = 17$), which will permit an analysis of peat initiation in a separate study. All samples were shipped to Bowdoin College and stored at 4°C until analysis.

2.3. Analytical Methods

Mineral samples were dried at 50°C for 48 hr, weighed to obtain a total dry mass, and sieved to obtain the mass of material >2 mm and <2 mm. The volume of the >2-mm fraction was estimated using volumetric displacement and was subtracted from the soil sampling cylinder volume to determine the volume of <2-mm soil. Fine fraction bulk density (<2 mm) was calculated to exclude rock content from the mineral soils. The root content of mineral soils was negligible; excluding the >2-mm root fraction in the estimates of bulk density had no significant effects on our measurements (data not shown).

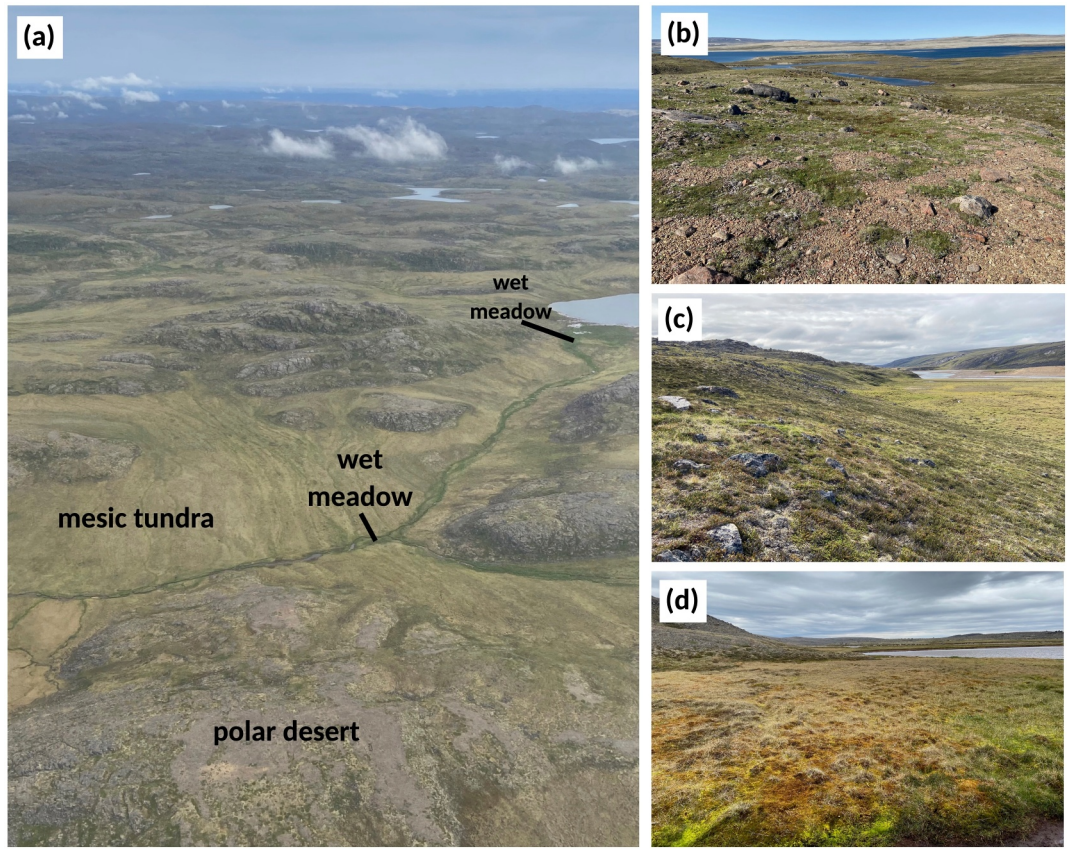

Figure 2. Representative tundra landscapes and ecosystems located in the study region on South Baffin Island: (a) Areal landscape photo showing varying topography and drainage network, with polar deserts (pink-gray color) on exposed hilltops, mesic tundra (yellow-green color) common on hillslopes, and wet meadow ecosystems (dark green color) occupying low-lying topographic positions near streams, ponds, and lakes, (b) polar desert ecosystem, (c) mesic tundra ecosystem, (d) *Sphagnum*-dominated wet meadow ecosystem (Photo credits: P. Camill).

The organic portion of the mesic tundra and wet meadow cores were dried at 50°C for 48 hr and then weighed. For the mesic tundra cores, bulk density of the organic layer was estimated by determining the volume of the monolith sampled in the field. The wet meadow cores were sampled for bulk density at 1–2-cm intervals for the portion of the core above the permafrost. Sampling intervals for the permafrost portion were determined by the depth of soil recovered by the permafrost corer. For each interval, a known volume was sampled using a 5-cc syringe. Each sample was dried at 50°C for 48 hr and then weighed. For all soils, bulk density is expressed as g-soil cm^{-3}. Percent and total C and N were measured using elemental combustion (Camill et al., 2017). Dried soil samples were ground in a SPEX SamplePrep 8000D ball mill to analytical fineness. Ground soils were analyzed for % C and % N using a CHNS elemental analyzer (Costech, Valencia, CA, USA). The molar C:N ratio was determined for each soil interval. Total C (kg-C m^{-2}) was calculated using the following equation:

$$\text{Total C} = \text{BD} \times \%\text{C}/100 \times D \times 10$$

where BD = soil bulk density (g-soil cm^{-3}), D = sampling depth interval (cm), and 10 is a factor used for unit conversion (Michaelson et al., 1996). Total N (kg-N m^{-2}) was obtained with the same equation by substituting % N for % C.

2.4. Vegetation Classification and Upscaling

We developed a vegetation classification based on the three dominant vegetation types—polar desert, mesic tundra, wet meadow—with two additional land cover types, barren and water. The imagery selected for vegetation classification was 10-m resolution Sentinel-2 images for summer months (July–September) for 2019–2023.

Table 1
Description of Vegetation Types Used in Field Sampling and Vegetation Classification

Cover type	Common species	Description	Soil properties/lithology
Polar Desert	*Vaccinium uliginosum*, *Vaccinium vitis-idaea*, *Dryas integrifolia*, *Oxytropis maydelliana*, true mosses, lichens	Sparsely vegetated with shrubs, herbs, and lichen crusts with patches of exposed mineral soil; occupied the higher and drier parts of the landscape, often on hilltops	Thin-to-no surface layer of organic material with rocky mineral soil below
Mesic Tundra	*Salix spp*., *Betula glandulosa*, *Cassiope tetragona*, *Rhododendron tomentosum*, true mosses, *Pleurozium schreberi*, *Vaccinium uliginosum*, *Vaccinium vitis-idaea*, *Arctostaphylos uva-ursi*, *Empetrum nigrum*, *Carex spp*.	Continuous vegetation cover with mixed species composition, including shrubs, herbs, and graminoids, with mosses appearing sporadically; often located on sloped terrain; intermediate in moisture	Surface organic layer with mineral soil appearing at depth (mostly <10 cm)
Wet Meadow	*Carex spp*., *Sphagnum spp*., *Salix spp*.	Dominated by sedges and peat-forming mosses; found in wet, low-lying areas; often adjacent to streams, ponds, and lakes	Predominantly organic material to depth, with the exception of river terrace sites receiving additional alluvial mineral inputs; variable organic layer depths ranging from 10 to 150 cm

Note. Adapted from Edwards and Treitz (2017).

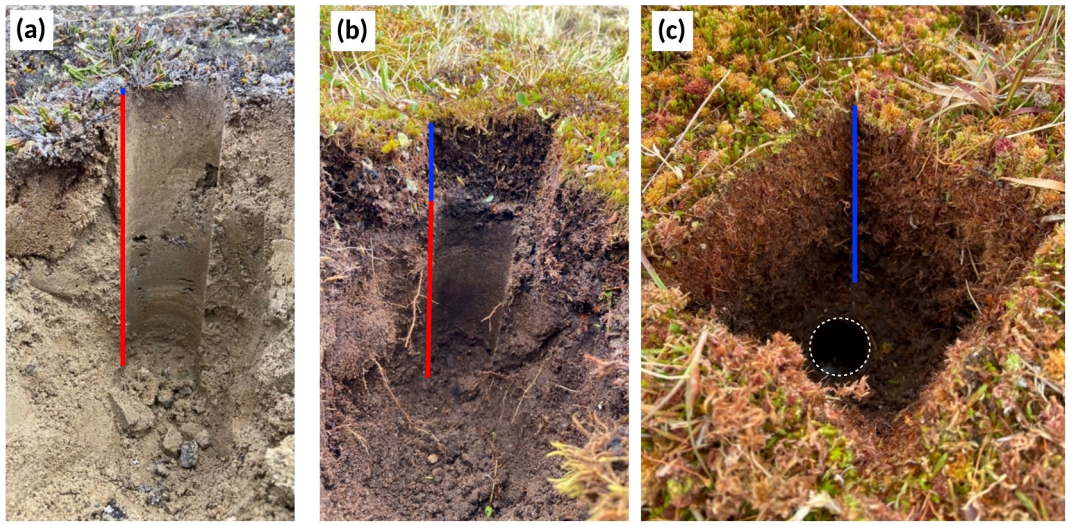

Figure 3. Soil structure for 0–20 cm depth varies considerably across the three major ecosystem types (blue line denotes thickness of organic layer; red line indicates thickness of mineral soil): (a) the polar desert soil profile was almost exclusively mineral soil, and the O-horizon was generally <1 cm thick; (b) mesic tundra had an organic epipedon overlying mineral soil; (c) wet meadow soil was commonly organic peat to depth. Permafrost peat was sampled from the bore hole (outlined by the dashed white circle) seen at the bottom of the surface core (Photo credits: P. Camill).

Google Earth Engine (Gorelick et al., 2017) was used to obtain 41 images atmospherically corrected (level 2A) to surface reflectance. To add barren land to the original data set of the 51 core locations, we used high-resolution imagery in Google Earth to locate equivalent points representing barren land cover across the study region (total $n = 68$). The coordinates and associated land cover types were uploaded into Google Earth Engine. Before beginning the land cover classification, we used the Normalized Difference Water Index (NDWI) to exclude water (McFeeters, 1996). The masked water layer was re-added to the map after the classification of non-water areas. For the remaining four land cover types, the average reflectance across 10 spectral bands (1, 2, 3, 4, 5, 6, 7, 8, 8A, 12) and 41 images for each vegetation type were used to create a training (80% of samples) and test (20% of samples) data set in Google Earth Engine. We used the training data set to train a Random Forest classifier (Breiman, 2001) with five trees, a minimum leaf population of one, and a bag fraction of 0.5. To evaluate the classification, we conducted an accuracy assessment using a resubstitution error matrix (Stehman, 1997). The resubstitution error matrix randomly removed a 20% out-of-bag test subsample to assess the overall accuracy of the classification (Stehman, 1997). Accuracy was expressed as a percent, with 100% accuracy representing a classifier where all test subsamples were identified correctly.

The land cover classification was used to spatially upscale ecosystem C based on the observed relationship between vegetation and soil C. To make our results comparable to estimates from the NCSCD, SoilGrids, and C-Band SAR, we standardized our core depth to the same depth as these databases (30 cm) (Bartsch et al., 2016; Hugelius et al., 2014; Poggio et al., 2021). For the wet meadow cores, which were collected to an average depth of 40 cm, only the average total C in the top 30 cm was calculated and used in this analysis. For the mesic tundra and polar desert cores, which were only sampled to a depth of 20 cm, we extrapolated soil C to a depth of 30 cm by assuming that total C storage in the 20–30 cm depth interval is the same as the 10–20 cm interval. The C storage of barren and water land cover types was assumed to be 0 kg m^{-2} due to the lack of soil development in these systems. Average total C (kg m^{-2}) for the top 30 cm was multiplied by the aerial land cover (km^2) for each vegetation type. The sum of C stored in each vegetation type produced the estimate for ecosystem C storage (reported in Tg C).

To evaluate CAVM as a potential circumpolar upscaling method, the vegetation map layer was downloaded and clipped to the study region (CAVM Team, 2022; Hugelius et al., 2013). For the 1-km raster CAVM, the 10 vegetation types present on South Baffin Island were grouped into the three predominant vegetation types (plus barren land cover) adapted in this study (Table 1). In general, there was a close match between the 10 cover types in CAVM and the four land cover types we selected (Table S1 in Supporting Information S1). The one exception

was CAVM polar desert cover class P2—prostrate/hemi-prostrate dwarf-shrub, lichen tundra. This class was defined broadly to include ecosystems with 40%–100% vegetation cover, which meant that it was functionally intermediate between polar desert ecosystems (sparsely vegetated) and mesic ecosystems (continuously vegetated). To account for the uncertainty associated with the P2 cover class, we generated two versions of the reclassified CAVM to account for differences in classifying this transitional vegetation type between polar desert and mesic tundra. In the first version of our analysis (CAVM 1), P2 was classified as polar desert, and in the second version (CAVM 2), P2 was classified as mesic tundra. Ecosystem soil C stocks based on the two CAVM versions were generated from the vegetation map and the new soil C data from this research.

Finally, the soil C upscaling approaches—NCSCD, SoilGrids, and C-Band SAR—were prepared for comparison. All three data layers representing soil C in the top 30 cm were downloaded and clipped to the study region. Ecosystem C storage for the NCSCD, SoilGrids, and C-Band SAR were estimated by multiplying their soil C values by the area occupied by each soil C data point in the three respective sources.

2.5. Statistical Methods

Mean differences in soil properties were analyzed using two-way ANOVA with post-hoc multiple comparison of means implemented in R v.4.3.1 (R Core Team, 2023). Vegetation type and depth were treated as fixed effects, and data were natural log transformed prior to analysis. Because multiple comparisons of means inflate the rate of type 1 error, Bonferroni corrections were made, and significance was assessed at the level of $\alpha = 0.0033$. Because of the large geographic distances among sites, we assume that the data are spatially independent.

The distribution of each soil property was also examined across vegetation types and depths using parametric and nonparametric modeling. Sample data were fit with a continuous probability density (normal, Weibull, gamma) using maximum likelihood estimation with package *fitdistrplus* (v.1.1–11) in R. Models were scaled to counts (rather than frequency) in order to plot them together with histograms of the data, and best-fit models were chosen using AIC statistics. A nonparametric assessment of differences in mean values for each soil property across vegetation types and depths was conducted using bootstrap resampling ($n = 10{,}000$) implemented with package *mosaic* (v.1.9.0) in R to generate bootstrap distributions of sample means and 95% confidence intervals.

3. Results

3.1. Soil Physical and Biogeochemical Properties

Soil organic matter depths were significantly different across vegetation types (Figures 3 and 4a, Figures S1a and S2a in Supporting Information S1, $p < 0.0001$). Organic depth in polar desert soils was too thin to measure accurately (consistently less than 1 cm), often consisting of a surficial lichen crust of variable thickness. In mesic tundra, mean organic layer depth was 6.91 ± 0.91 cm. The wet meadow organic layers were the deepest and most variable (mean = 40.12 ± 8.11 cm, with a range of 10–151 cm).

Bulk density varied across both vegetation type and depth (Figure 4b, Figures S1b and S2b in Supporting Information S1), with a significant interaction existing between vegetation type and depth ($p = 0.012$). Polar desert soils dominated by mineral soil across the 0–20-cm soil profile (Figure 3a) showed greater bulk density (1.18 ± 0.06 g-soil cm^{-3}), compared to organic-rich, low-bulk-density wet meadow soils (0.21 ± 0.02 g-soil cm^{-3}). Deeper mesic tundra soils (10–20 cm) were also high bulk density (1.074 ± 0.09 g-soil cm^{-3}) and were not significantly different than polar desert soils because of the predominance of mineral soil ($p = 0.258$). Soils in the surface (0–10 cm) layer of mesic tundra showed an intermediate bulk density (0.492 ± 0.05 g-soil cm^{-3}) that differed significantly from both the polar desert and wet meadow soils ($p < 0.0001$).

Percent C was inversely related to soil mineral content and bulk density across the three vegetation types (Figure 4c, Figure S3 in Supporting Information S1). Similar to bulk density, both vegetation type and soil depth were explanatory variables, but a significant interaction existed between them ($p < 0.0001$) (Figures S1c and S2c in Supporting Information S1). In the 0–10-cm layer, percent C was significantly different across the vegetation types (Figure 4c): lowest in the polar desert (1.47% ± 0.32), intermediate in mesic tundra (23.19% ± 2.73), and highest in the wet meadow (41.63% ± 1.18). A similar trend was observed at the 10–20-cm depth: polar desert (0.66% ± 0.20) < mesic tundra (5.74% ± 2.79) < wet meadow (33.24% ± 2.56). All three vegetation types showed a decline in percent C from 0–10 cm to 10–20 cm, with the difference only being significant in mesic tundra soils ($p < 0.0001$).

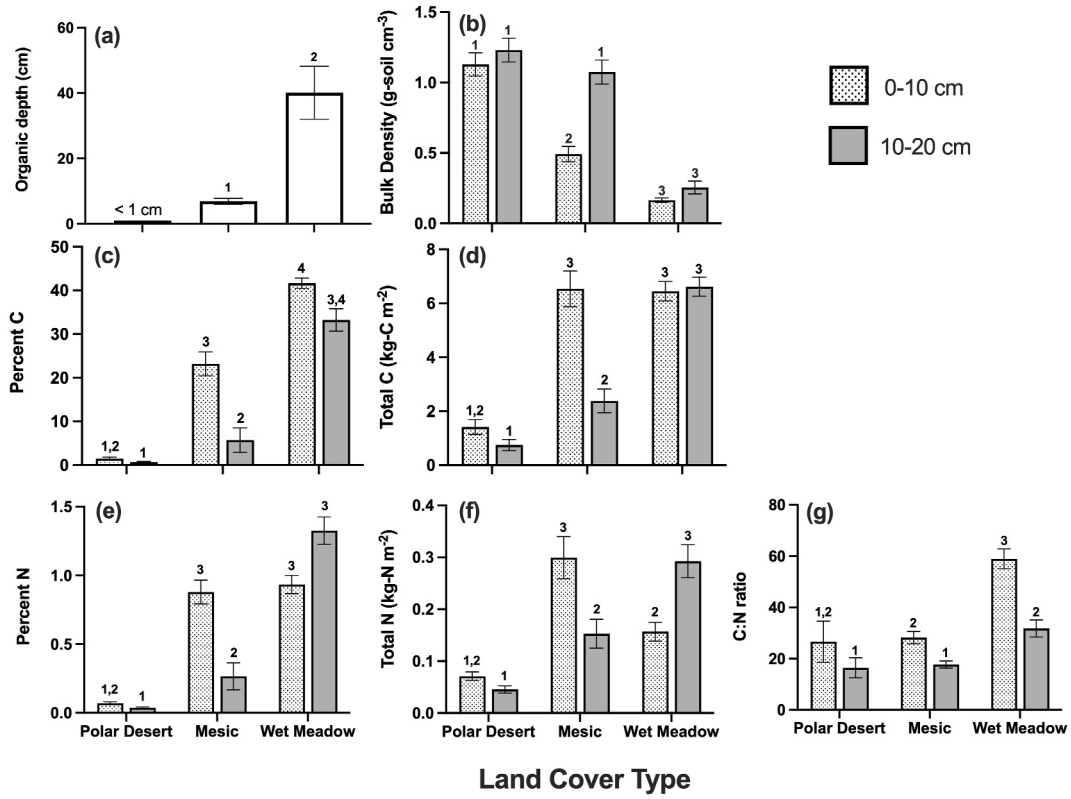

Figure 4. Soil properties measured for each vegetation type: (a) mean organic depth (cm), (b) mean bulk density (g-soil cm^{-3}), (c) mean percent C (%), (d) mean total C (kg-C m^{-2}), (e) mean percent N (%), (f) mean total N (kg-N m^{-2}), (g) mean molar C:N ratio. Stippled and solid gray bars represent data for the 0–10 and 10–20-cm soil layers, respectively. Error bars represent ±1 standard error of the mean. Numbers above the bars denote significance based on post-hoc mean comparisons with Bonferroni corrections ($\alpha = 0.0033$). Post-hoc mean comparisons were not performed with the polar desert organic depth due to the difficulty of measurement.

In the top 20 cm, total C amounted to 2.17 ± 0.48 kg-C m^{-2} in polar desert, 8.92 ± 0.74 kg-C m^{-2} in mesic tundra, and 13.07 ± 0.69 kg-C m^{-2} in wet meadow. Similar to both bulk density and percent C, total soil C was affected by vegetation type and soil depth, although a significant interaction existed between them ($p = 0.0005$) (Figure 4d, Figures S1d and S2d in Supporting Information S1). In the top 10 cm, there was no significant difference between the total C stored in the organic-rich mesic tundra and wet meadow soils ($p = 0.758$, Figures 3b and 3c), with mean total C values of 6.54 ± 0.66 kg-C m^{-2} and 6.45 ± 0.36 kg-C m^{-2}, respectively. Mean total soil C at the 0–10 cm depth was significantly lower in the mineral-rich polar desert (1.42 ± 0.28 kg-C m^{-2}). However, in the 10–20-cm soil depth, there was a significant difference in total soil C across all three vegetation types, with wet meadow > mesic tundra > polar desert (Figure 4d, $p < 0.0002$). Wet meadow soils at depth (6.62 ± 0.35 kg-C m^{-2}) had a statistically similar mean total C to the top 10 cm ($p = 0.702$). In contrast, mesic tundra total C (2.38 ± 0.44 kg-C m^{-2}) and polar desert total C (0.75 ± 0.21 kg-C m^{-2}) declined by over half compared to the surface 0–10 cm depth, although the difference was significant only in mesic tundra ($p < 0.0001$).

Total N stocks in the top 20 cm were 0.12 ± 0.1 kg-N m^{-2} in polar desert, 0.45 ± 0.5 kg-N m^{-2} in mesic tundra, and 0.44 ± 0.05 kg-N m^{-2} in wet meadow. Soil N showed trends similar to soil C, but important differences existed (Figures 4e–4f, Figures S1e and S1f, S2e and S2f in Supporting Information S1). Percent N was related to both vegetation type and depth (Figure 4e, $p < 0.0001$), and a significant interaction existed between these factors ($p < 0.0001$). In both soil depths, percent N followed the same trend as percent C for the polar desert and mesic tundra soils. A notable difference occurred with the wet meadow soils, where, unlike percent C, percent N was lower in the surface soils (0.93% ± 0.07) than at depth (1.33% ± 0.10) (Figure 4e). Total soil N was significantly related to vegetation type ($p < 0.0001$) but not depth ($p = 0.051$), and an interaction existed between these factors (Figure 4f, $p < 0.0001$). Similar to percent N, the trend in total N was similar to total C for polar desert and mesic

Table 2
Percent Landscape Cover and Accuracy for Vegetation Classification

Land cover type	Percent of landscape	Percent accuracy
Barren	42.2	91.2
Polar Desert	28.8	93.9
Mesic Tundra	9.8	88.4
Wet Meadow	1.6	89.8
Water	17.6	N/A

tundra soils, but the size of the soil N pool reversed for the wet meadow soils, with surface soils storing significantly lower total N (0.16 ± 0.02 kg-N m^{-2}) than at depth (0.29 ± 0.03 kg-N m^{-2}) ($p = 0.0009$).

Molar C:N ratios differed across both vegetation type ($p < 0.0001$) and soil depth ($p < 0.0001$), and, unlike bulk density, percent/total C, and percent/total N, the interaction between these factors was not significant ($p = 0.587$) (Figure 4g, Figures S1g and S2g in Supporting Information S1). Across the entire soil profile, C:N ratio was greater in wet meadow compared to polar desert and mesic tundra soils, and there was no significant difference between polar desert and mesic tundra soils at either depth ($p > 0.1$). The C:N ratio declined with depth in all vegetation types, although the decrease was significant only for mesic tundra ($p = 0.0002$) and wet meadow ($p < 0.0001$) soils.

3.2. Landscape Classification

The landscape in the study region was dominated by barren, polar desert, and water, with a sparse cover of mesic tundra and wet meadow (Table 2). The overall classification accuracy was 90.7%. The classification of polar desert land was most accurate, followed by barren, wet meadow, and mesic tundra. The accuracy of water was not assessed because it was pre-classified in Google Earth Engine and then re-added to the map. A comparison of Sentinel-2 imagery and our classification at the site level can be found in the supplemental materials (Figure S4 in Supporting Information S1).

The map of the study region classified by land cover type shows trends in the distribution of each vegetation type (Figure 5a). The barren cover was predominantly concentrated in two linear (mountainous terrain) features along the long edges of the study region. The polar desert cover occupied the majority of the space between the two barren features. Within the polar desert cover, both the mesic tundra and the wet meadow appeared, at both broad and fine scales, around water bodies—rivers, lakes, and Frobisher Bay (Figure 5, Figure S4 in Supporting Information S1).

Our vegetation classification yielded estimates of vegetation cover that differed from the two versions of the 1-km resolution CAVM classification (Figures 5b and 5c) (CAVM Team, 2022). Both versions of CAVM produced a more barren landscape than our classification, although CAVM differed slightly in the locations of barren land cover (Table 3, Figures 5b and 5c). The percent wet meadow cover was the same in all three classifications despite a more spatially clustered distribution in CAVM as compared to a patchier distribution in ours (see Figure S4 in Supporting Information S1). Polar desert and mesic tundra cover in our classification fell in the middle of estimates from CAVM 1 and CAVM 2 (Table 3). CAVM 2 appears more similar to our classification (Figures 5a–5c).

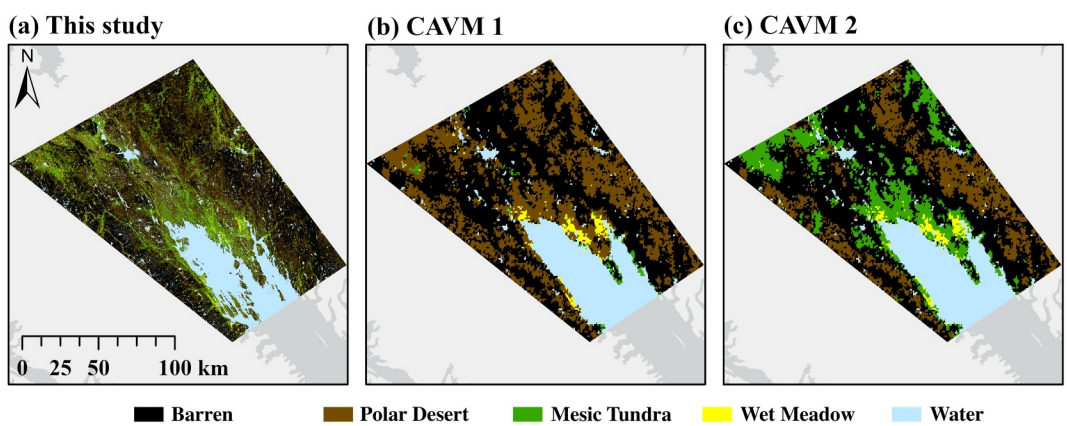

Figure 5. Comparison between (a) land cover classification of this study, (b) CAVM 1, (c) CAVM 2 (adapted from CAVM Team, 2022). In CAVM 1, the original CAVM P2 land cover class (prostrate/hemi-prostrate dwarf-shrub, lichen tundra) was classified as polar desert, while CAVM 2 classified P2 as mesic tundra.

Table 3
Comparison of Percent Land Cover From This Study and From CAVM

Land cover type	Percent of landscape (this study)	Percent of landscape (CAVM 1)	Percent of landscape (CAVM 2)
Barren	42.2	48.0	48.0
Polar Desert	28.8	32.6	15.6
Mesic Tundra	9.8	1.1	16.7
Wet Meadow	1.6	1.6	1.6
Water	17.6	16.6	16.6

Note. Original CAVM land cover types were clipped to the study region and re-classified into the four land cover types in this study.

3.3. Regional C Stocks

Extrapolating total C to a depth of 30 cm yielded results of 2.91 kg-C m^{-2} for polar desert, 11.30 kg-C m^{-2} for mesic tundra, and 20.02 kg-C m^{-2} for wet meadow ecosystems. Scaling these values to the entire region using the land cover classification (Figure 6a) indicated that high C storage was located in proximity to water bodies, where the mesic tundra and wet meadow land cover types were more common (Figures 2, 5a, and 6a). Mean landscape soil C stock was 2.27 ± 0.37 kg-C m^{-2} for the whole study region and 2.75 ± 0.45 kg-C m^{-2} when excluding water areas.

Comparing upscaled soil C stock estimates in the top 30 cm of soil from this study to previously published efforts to map vegetation and upscale soil C, we note substantial differences among the approaches. By applying the soil C storage estimates from this study to two CAVM vegetation maps, we estimated a C inventory of 27.3 Tg C for CAVM 1 and 52.9 Tg C for CAVM 2 (Figures 6b and 6c, Table 4). The soil C inventories from the NCSCD and SoilGrids assessment were both significantly higher: 189.8 and 127.9 Tg C, respectively (Figures 6d and 6e, Table 4). The C-Band SAR approach resulted in a lower estimate of 80.9 Tg (Figure 6f) (Table 4). Our upscaling estimate in this study lies in the lower end of this range: 44.2 ± 7.3 Tg C (Figure 6a, Table 4).

4. Discussion

South Baffin Island appears to support significant accumulation of soil C that is spatially variable as a function of vegetation type and, at the landscape scale, topography and hydrology (Figures 2–4d, and 6a, Figures S1 and S2 in Supporting Information S1, Table 4). Because vegetation cover can be mapped effectively using remotely sensed data (Figure 5a), vegetation-based upscaling is an effective method of representing surface soil C. To the extent that efforts to upscale circumpolar soil C stocks do not account for the significant relationship between vegetation and soil C at finer spatial scales, these inventories may be under or overestimating high-latitude soil C storage and could benefit from the inclusion of explicit accounting of vegetation-soil C interactions. While vegetation-based upscaling may only accurately represent surface soil layers up to 30 cm depth, this methodology is sufficient for shallow high arctic soils.

Comparisons in soil C estimates across the Arctic are challenged by differences in soil sampling techniques, depths, and upscaling methods (Horwath Burnham & Sletten, 2010). Despite these challenges, comparisons can be made between our mean landscape soil C estimate (2.75 ± 0.45 kg m^{-2}; depth = 30 cm) and a sample of other regions. South Baffin Island is moderate in soil C as compared to nearby landscape-level measurements in NE Greenland (1.9 kg m^{-2}; depth = 30 cm), NW Greenland (9.0 kg m^{-2}; depth = 1 m), Svalbard (2.7 kg m^{-2}; depth = 30 cm) and northern Sweden (3.9 kg m^{-2}; depth = 30 cm) (Horwath Burnham & Sletten, 2010; Palmtag et al., 2018; Siewert, 2018; Wojcik et al., 2019). However, South Baffin Island soil C stocks are low in comparison to regions like Alaska and Russia. Johnson et al. (2011) estimated a mean landscape soil C storage of 44.0 kg m^{-2} (440 Mg ha^{-1}) for the top 1 m for the entire Arctic Tundra region. Studies in Russia have also reported a range of higher soil C values from 11 to 30.7 kg m^{-2} to a depth of 1 m (Gundelwein et al., 2007).

The interplay between percent C and bulk density illustrate how soil properties are inherited from vegetation types and control the size of the total C stored in each vegetation type. Vegetation composition and biomass can affect the amount of plant litter produced, and C quality affects the rate of decomposition of the organic matter (Atkinston & Treitz, 2012; Bradley-Cook & Virginia, 2018; Lamarque et al., 2023; Mekonnen, Riley, Grant, et al., 2021). This is most pronounced in the study region in comparing the sparsely vegetated polar desert soils to

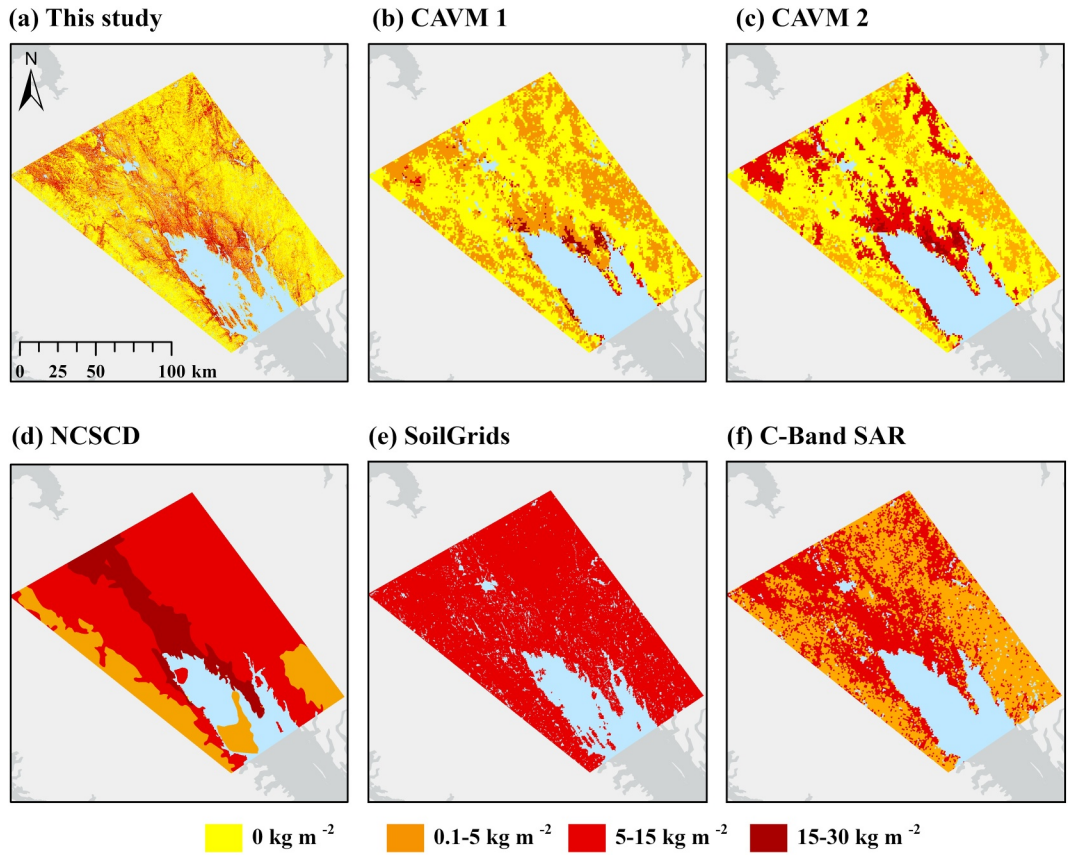

Figure 6. Map of C stocks in the top 30 cm in the study region upscaled for (a) this study, (b) CAVM 1 (CAVM team, 2023), (c) CAVM 2 (CAVM team, 2022), (d) NCSCD (Hugelius et al., 2013), (e) SoilGrids (Poggio et al., 2021), and (f) C-Band SAR (Bartsch et al., 2016).

the ecosystems having continuous vegetation cover, the mesic tundra and wet meadow soils. Throughout the soil profile, the polar desert vegetation exhibited denser mineral soils (Figures 3a and 4b). However, because of the sparse vegetation cover, polar desert soils have very low percent C (Figure 4c), and thus do not accumulate significant soil C pools (Figure 4d). In contrast, the wet meadow soils have the lowest density (Figure 4b), but store significant amounts of C due to the high percent C inherited from *Sphagnum* peat (Figures 3c, 4c and 4d, Loisel et al., 2014). A similar tradeoff between percent C and bulk density (Figure S3 in Supporting Information S1) has been observed throughout the arctic (Hossain et al., 2015). Our work indicates that vegetation type is an important factor in explaining this relationship. Polar desert (high bulk density and low % C) and wet meadow (low bulk density and high % C) cores represent the end members of this relationship, whereas mesic tundra had moderate density and moderate percent C (see Figure S3 in Supporting Information S1).

Table 4
Ecosystem C Stocks Reported for Each Classification Source

Source	Upscaled C stock estimate (Tg)
CAVM 1	27.3
CAVM 2	52.9
This Paper	44.2 ± 7.3
NCSCD	189.8
SoilGrids	127.9
C-Band SAR	80.9

Soil depth is another important factor to consider when examining the relationship between vegetation type, bulk density, percent C, and total soil C (Figure 4). As noted above, polar desert and wet meadow cores show less variation in bulk density, percent C and total C in the top 20 cm (Figures 4b–4d) because the polar desert cores were mainly mineral soil and the wet meadow cores were mainly organic soil (Figure 3). Because of the organic epipedon overlying mineral soil in mesic tundra ecosystems (Figure 3b), it was not surprising to find that mesic tundra soils from 0 to 10 cm exhibited biogeochemical properties similar to surficial wet meadow soils (Figure 4, Figures S1 and S2 in Supporting Information S1), whereas soils from 10 to 20 cm were more similar to mineral-dominated polar desert ecosystems (Figure 4, Figures S1 and S2 in Supporting Information S1).

The patterns of soil N in this arctic landscape appear to be influenced by vegetation and soil C. For polar desert and mesic tundra sites, percent and total N followed the trends of soil C closely (Figures 4c–4f). This is not surprising given that C and N are abundant elements in organic matter (Sterner & Elser, 2002). In the wet meadow ecosystem, however, soil N trends diverged from soil C (compare Figures 4d–4f). Total soil N was lower in the surface soil relative to depth, and this trend correlated with significantly higher C:N ratios in the surface soil layer of wet meadows (Figure 4g). We speculate that lower N in wet meadow surface soils could be caused by a number a factors: higher fraction of woody tissues, N uptake and storage in aboveground biomass, or possibly higher rates of denitrification (K. A. Edwards & Jefferies, 2010; Hung et al., 2023; Weintraub & Schimel, 2003). Lower C:N ratios and lower soil C stocks in polar desert and mesic tundra soils suggest higher-quality litter fosters higher decomposition rates (Lynch et al., 2018). Meanwhile, the higher C:N ratio of the organic matter in wet meadow soils may be less decomposable, leading to the development of greater C stocks at depth (Bradley-Cook & Virginia, 2018).

Hydrology is also an important factor in the development of soil C pools in this region. The exposed, well-drained soils of polar desert ecosystems likely inhibited plant production and facilitated soil decomposition, which would prevent the accumulation of large soil C pools. In contrast, the low-lying, wet conditions of the wet meadow ecosystems supported the growth of sedges and peat mosses, and the wet conditions also likely inhibited decomposition (Hicks Pries et al., 2013; McGuire et al., 2009), thus leading to larger soil C pools in these ecosystems. Peat accumulation in the wet meadow sites was often significant; peat depths greater than 20 cm only occurred in the wet meadow ecosystems.

Results from this study contribute to a growing awareness that the relationship between vegetation type and soil C appears to vary across regions of the Arctic. Prior work in Greenland suggests agreement with our finding that soils underlying graminoid-dominated vegetation (our wet meadow sites) store more C than shrub-dominated vegetation (our mesic tundra and polar desert sites) (Bradley-Cook & Virginia, 2018; Petrenko et al., 2016). However, other work from Greenland found that arctic ecosystems dominated by tall shrubs or wet shrub areas fed by snow beds stored more C than graminoid soils (Elberling et al., 2004; Gries et al., 2020). Given limited data for how vegetation types affect soil C storage in the Arctic, it is clear that more research is required to understand this relationship.

Despite variations in the relationship between vegetation and soil C across the Arctic, understanding the local relationship between vegetation and soil C is beneficial for predicting the impacts of climate change on South Baffin Island. If warming results in the expansion of mesic tundra vegetation into polar desert regions, ecosystem soil C storage will increase. The future of precipitation may control the fate of wet meadow ecosystems, with increased precipitation and wetting resulting in the expansion of peat systems. However, if wet meadow areas dry and are overtaken by mesic tundra vegetation, ecosystem soil C storage will decrease.

In addition to better understanding the relationship between vegetation and soil C, efforts to upscale local soil C measurements to regional C inventories require accurately described vegetation classes. Due to differences in vegetation classifications, ecosystem C estimates from CAVM versions differ sharply from each other. CAVM 2 estimate (52.9 Tg C) represents an almost 100% increase compared to CAVM 1 (27.3 Tg C). This discrepancy highlights the importance of correctly classifying transitional vegetation types, such as the CAVM class P2, which may be intermediate between two major vegetation types (polar desert and mesic tundra) that differ significantly in soil C storage (Figure 4e). Although the CAVM land cover P2 is classified as polar desert (Table S1 in Supporting Information S1), it is more spatially coherent with our results when classified as mesic tundra (CAVM 2) rather than polar desert (CAVM 1) (compare Figures 5a–5c). Because of strong links between vegetation type and soil C (Figure 4e), differences in the percent cover of vegetation types results in large differences in ecosystem C storage.

Additional attention to spatial scale of land cover classifications also can improve efforts to assess and upscale arctic soil C stocks. Regardless of which vegetation classification was used, both versions of CAVM generated ecosystem C estimates that vary from the results of this study, either underestimating by 17 Tg C (CAVM 1) or overestimating by 8 Tg C (CAVM 2) relative to our results (Table 4). Higher-resolution imagery is beneficial for two important reasons in the Arctic: (a) It permits the identification of local streams and ponds (and associated C-rich mesic and wet meadow ecosystems), and (b) it may better represent ecosystems that respond strongly to landscape variation. Although the overall percent cover of wet meadow is the same between our classification and CAVM, the distribution of this ecosystem type across the landscape in association with streams, ponds, and lakes

is less well described at the 1-km CAVM resolution (Figure 5) and is often poorly described at the site scale (Figure S4 in Supporting Information S1). Both CAVM classifications may misrepresent the land cover of mesic tundra and polar desert because of the difficulty to assessing how these ecosystems respond to topographic variability at scales finer than 1-km resolution (Figure S4 in Supporting Information S1). Our classification may better assess this variability as well as transitions between these two vegetation types, resulting in estimates of polar desert, mesic tundra, and soil C that fall between the two CAVM classifications for the study region. Our results indicate that the spatial distribution of land cover types and regional soil C stocks can be improved with the use of 10-m resolution imagery. To the extent that C-rich ecosystems, such as wet meadow and mesic tundra, are distributed throughout the landscape in response to finer-scale topographical and hydrological changes, this could have implications for the rate of high-Arctic response to climate warming/wetting if small, patchy, distributed ecosystems respond more rapidly than large, clustered ecosystems. While other research suggests that even 1-m or cm-level resolution is required to represent variable arctic environments, improving the resolution of upscaling approaches may be more limited by the lack of sufficient soil carbon data than the availability remote sensing products (Räsänen et al., 2019; Siewert, 2018; Yang et al., 2021).

Higher-resolution soil C measurements directly linked to dominant vegetation types also provide an opportunity to improve circumpolar upscaling efforts. Approaches to capture soil C like the NCSCD, SoilGrids, C-Band SAR are meant to be highly generalized, which may explain some variation in local level soil C estimates. Even so, our analysis generated a regional soil C stock estimate (44.2 Tg C) that was only 23% of the value reported for the NCSCD (189.4 Tg C) (Hugelius et al., 2014) (Table 4). When examined at the local scale, the soil pedons fail to capture the heterogeneity of the landscape, and the soil C stocks attributed to each soil pedon are too high (Figure 6d). This may be caused by uneven distribution of soil profiles in the NCSCD: A disproportionate amount of soil C data come from C-rich regions like Alaska and Siberia (Hugelius et al., 2014). The SoilGrids estimate for the study region was only slightly lower than the NCSCD (127.9 Tg C) (Table 4). While SoilGrids has the highest resolution of the three databases, there is little variation in soil C stocks captured in each 250-m × 250-m pixel, and the soil C values are high (Figure 6e). Similar to the NCSCD, the lack of variability and high stocks may arise from insufficient soil data and the limited sample points representing higher-C environments than Baffin Island (Poggio et al., 2021). Finally, the C-Band SAR approach yielded an ecosystem soil C estimate (80.9 Tg) closest to our own and identified a similar spatial distribution of soil C throughout the study region (Table 4; Figures 6a and 6f). While the C-Band SAR methodology could improve with higher-resolution imagery, the approach benefits from direct measurements of surface characteristics and assigning the correlated C value to each raster pixel, and thus is more spatially consistent than other methodologies (Bartsch et al., 2016). Nevertheless, their soil C estimates are still higher than reported in this study. One explanation may be that the correlations between SAR values and soil C stocks were generated from high-resolution data from five sites in the Arctic, four of which had higher mean landscape soil C stocks than this study (Hugelius et al., 2010; Palmtag et al., 2015, 2016; Siewert et al., 2015).

5. Conclusion

Arctic vegetation types have a significant impact on the size of surface soil C stocks on South Baffin Island. Soil properties like organic layer depth, bulk density, and percent C mediate the link between vegetation type and soil C. Vegetation, in turn, is controlled by landscape-level features, including topography and moisture. Determining the relationship between vegetation and soil C is an asset for mapping and upscaling soil C in the Arctic because it permits the use of remotely sensed data to predict subsurface soil C based on representative vegetation mapping and soil C stocks. High-resolution vegetation mapping of the study region reveals a greener landscape than estimated by prior coarse-scale vegetation maps. Future shrubification and peat expansion may continue to occur on a patchy scale because the Arctic is spatially heterogeneous. Thus, analyses at finer scales are recommended in order for vegetation mapping to account for surficial variability. Additionally, circumpolar soil C databases are limited by the distribution of soil data, and increasing research in understudied regions will improve our estimates of pan-arctic soil C stocks.

Global Research Collaboration

This work was completed in compliance with terms and conditions specified by the Nunavut Impact Review Board, the Department of Culture & Heritage, and the scientific research license issued by the Nunavut Research Institute. We are grateful for additional assistance with field logistics from H. Ell and A. Flaherty with Polar Outfitting.

Data Availability Statement

The NCSCD data are available for download on the Bolin Centre Database at Stockholm University (https://bolin.su.se/data/ncscd/). The Raster CAVM (v2) data are available on the Alaska Geobotany Center from University of Alaska Fairbanks (https://www.geobotany.uaf.edu/cavm/). SoilGrids data are available on the SoilGrids website (https://soilgrids.org/). The data from the C-Band SAR method are available at https://doi.pangaea.de/10.1594/PANGAEA.864712 (Bartsch et al., 2016). Google Earth Engine was used to obtain Sentinel-2 imagery, run a supervised classification for vegetation, and process the outside data sources. The Google Earth Engine Code for the vegetation classification is accessible here with registration for a free account. Original data and code from this study are archived publicly at the National Science Foundation Arctic Data Center under Gunther et al. (2024) (https://doi.org/10.18739/A29Z90D69).

Acknowledgments

We express deep gratitude to the Inuit communities of Nunavut, Baffin Island, and the Iqaluit region for the opportunity to study their ancestral lands. Funding for this research was provided by the National Science Foundation (NSF) under grant NNA: Collaborative Research: MSB-FRA: 1802732. Any opinions, findings, and conclusions or recommendations expressed are those of the authors and do not necessarily reflect the views of the NSF. This research would not have been possible without logistical support provided by the following individuals: S. Caron, H. Ell, A. Flaherty, F. Bernadac, J. Stoddard, Ri. Armstrong, M. Cote, G. Djalogue, and S. LeBlanc. We are grateful for additional support provided by M. Melendy, B. Spaeth, E. Kallin, Ro. Armstrong, J. Kelley, M. Hart, L. Pilgrim, J. Anderson, S. Woodworth, M. Belyea, R. Bernier, and C. Wojtysiak.

References

Aide, M. T., Aide, C., & Braden, I. (2021). In S. Sarvajayakesavalu & P. Chareonsudjai (Eds.), *Soil genesis of histosols and gelisols with a emphasis on soil processes supporting carbon sequestration*. Environmental Issues and Sustainable Development. London, UK: IntechOpen.

Arndt, K. A., Santos, M. J., Ustin, S., Davidson, S. J., Stow, D., Oechel, W. C., et al. (2019). Arctic greening associated with lengthening growing seasons in Northern Alaska. *Environmental Research Letters*, *14*(12), 125018. https://doi.org/10.1088/1748-9326/ab5e26

Atkinston, D. M., & Treitz, P. (2012). Arctic ecological classification derived from vegetation community and satellite spectral data. *Remote Sensing*, *4*(12), 3948–3971. https://doi.org/10.3390/rs4123948

Bakian-Dogaheh, K., Chen, R. H., Yi, Y., Kimball, J. S., Moghaddam, M., & Tabatabaeenejad, A. (2022). A model to characterize soil moisture and organic matter profiles in the permafrost active layer in support of radar remote sensing in Alaskan Arctic tundra. *Environmental Research Letters*, *17*(2), 025011. https://doi.org/10.1088/1748-9326/ac4e37

Bartsch, A., Widhalm, B., Kuhry, P., Hugelius, G., Palmtag, J., & Siewert, M. B. (2016). Can C-band synthetic aperture radar be used to estimate soil organic carbon storage in tundra? *Biogeosciences*, *13*(19), 5453–5470. https://doi.org/10.5194/bg-13-5453-2016

Batjes, N. H., Ribeiro, E., & van Oostrum, A. (2020). Standardised soil profile data to support global mapping and modelling (WoSIS snapshot 2019). *Earth System Science Data*, *12*(1), 299–320. https://doi.org/10.5194/essd-12-299-2020

Bockheim, J. G. (1979). Properties and relative age of soils of Southwestern Cumberland Peninsula, Baffin Island, N.W.T., Canada. *Arctic and Alpine Research*, *11*(3), 289–306. https://doi.org/10.2307/1550418

Bradley-Cook, J. I., & Virginia, R. A. (2018). Landscape variation in soil carbon stocks and respiration in an Arctic tundra ecosystem, west Greenland. *Arctic Antarctic and Alpine Research*, *50*(1), S100024. https://doi.org/10.1080/15230430.2017.1420283

Breiman, L. (2001). Random forests. *Machine Learning*, *45*(1), 5–32. https://doi.org/10.1023/A:1010933404324

Broll, G., Tarnocai, C., & Mueller, G. (1999). Interactions between vegetation, nutrients and moisture in soils in the Pangnirtung Pass Area, Baffin Island, Canada. *Permafrost and Periglacial Processes*, *10*(3), 265–277. https://doi.org/10.1002/(SICI)1099-1530(199907/09)10:3<265::AID-PPP326>3.0.CO;2-K

Bruhwiler, L., Parmentier, F.-J. W., Crill, P., Leonard, M., & Palmer, P. I. (2021). The Arctic carbon cycle and its response to changing climate. *Current Climate Change Reports*, *7*(1), 14–34. https://doi.org/10.1007/s40641-020-00169-5

Camill, P., Umbanhowar, C. E., Jr., Geiss, C., Edlund, M. B., Hobbs, W. O., Dupont, A., et al. (2017). The initiation and development of small peat-forming ecosystems adjacent to lakes in the north central Canadian low arctic during the Holocene. *Journal of Geophysical Research: Biogeosciences*, *122*(7), 1672–1688. https://doi.org/10.1002/2016JG003662

Campbell, T. K. F., Lantz, T. C., Fraser, R. H., & Hogan, D. (2021). High Arctic vegetation change mediated by hydrological conditions. *Ecosystems*, *24*(1), 106–121. https://doi.org/10.1007/s10021-020-00506-7

CAVM Team. (2003). *Circumpolar Arctic vegetation map (conservation of Arctic flora and fauna (CAFF) map No. 1, 1:7,500,000 scale)*. U.S. Fish and Wildlife Service.

CAVM Team. (2022). *Raster circumpolar Arctic vegetation map (version 2. Scale 1:7,000,000)*. Mendely Data.

Chapin, F. S., III., Fetcher, N., Kielland, K., Everett, K. R., & Linkins, A. E. (1988). Productivity and nutrient cycling of Alaskan tundra: Enhancement by flowing soil water. *Ecology*, *69*(3), 693–702. https://doi.org/10.2307/1941017

Corbett, L. B., Bierman, P. R., & Davis, P. T. (2016). Glacial history and landscape evolution of southern Cumberland Peninsula, Baffin Island, Canada, constrained by cosmogenic 10Be and 26Al. *GSA Bulletin*, *128*(7–8), 1173–1192. https://doi.org/10.1130/B31402.1

Edwards, K. A., & Jefferies, R. L. (2010). Nitrogen uptake by *Carex aquat*ilis during the winter–spring transition in a low Arctic wet meadow. *Journal of Ecology*, *98*(4), 737–744. https://doi.org/10.1111/j.1365-2745.2010.01675.x

Edwards, R., & Treitz, P. (2017). Vegetation greening trends at two sites in the Canadian Arctic: 1984–2015. *Arctic Antarctic and Alpine Research*, *49*(4), 601–619. https://doi.org/10.1657/AAAR0016-075

Elberling, B., Jakobsen, B. H., Berg, P., Søndergaard, J., & Sigsgaard, C. (2004). Influence of vegetation, temperature, and water content on soil carbon distribution and mineralization in four high arctic soils. *Arctic Antarctic and Alpine Research*, *36*(4), 528–538. https://doi.org/10.1657/1523-0430(2004)036[0528:IOVTAW]2.0.CO;2

Environment Climate Change Canada. (2023). Canadian climate normals 1981-2010 station data: Iqaluit, Nunavut [Dataset]. *Government of Canada*. Retrieved from https://climate.weather.gc.ca/climatenormals/indexe.html

Evans, L. J., & Cameron, B. H. (1979). A chronosequence of soils developed from granitic morainal material, Baffin Island, N.W.T. *Canadian Journal of Soil Science*, *59*(2), 203–210. https://doi.org/10.4141/cjss79-020

Fisher, J. B., Hayes, D. J., Schwalm, C. J., Huntzinger, D. N., Stofferahn, E., Schaefer, K., et al. (2018). Missing pieces to modeling the Arctic-Boreal puzzle. *Environmental Research Letters*, *13*(2), 020202. https://doi.org/10.1088/1748-9326/aa9d9a

Ford, J. D., Couture, N., Bell, T., & Clark, D. G. (2017). Climate change and Canada's north coast: Research trends, progress, and future directions. *Environmental Reviews*, *26*(1), 82–92. https://doi.org/10.1139/er-2017-0027

Gagnon, M., Domine, F., & Boudreau, S. (2019). The carbon sink due to shrub growth on Arctic tundra: A case study in a carbon-poor soil in eastern Canada. *Environmental Research Communications*, *1*(9), 091001. https://doi.org/10.1088/2515-7620/ab3cdd

Gorelick, N., Hancher, M., Dixon, M., Ilyushchenko, S., Thau, D., & Moore, R. (2017). Google Earth engine: Planetary-scale geospatial analysis for everyone. *Remote Sensing of Environment*, *202*(1), 18–27. https://doi.org/10.1016/j.rse.2017.06.031

Gould, W. A., Raynolds, M., & Walker, D. A. (2003). Vegetation, plant biomass, and net primary productivity patterns in the Canadian Arctic. *Journal of Geophysical Research*, *108*(D2), 8167. https://doi.org/10.1029/2001JD000948

Gries, P., Schmidt, K., Scholten, T., & Kühn, P. (2020). Regional and local scale variations in soil organic carbon stocks in West Greenland. *Journal of Plant Nutrition and Soil Science*, *183*(3), 292–305. https://doi.org/10.1002/jpln.201900390

Gundelwein, A., Müller-Lupp, T., Sommerkorn, M., Haupt, E., Pfeiffer, E.-M., & Wiechmann, H. (2007). Carbon in tundra soils in the Lake Labaz region of arctic Siberia. *European Journal of Soil Science*, *58*(5), 1164–1174. https://doi.org/10.1111/j.1365-2389.2007.00908.x

Gunther, A., Camill, P., Umbanhowar, C., Stansfield, A., & Dethier, E. (2024). *Vegetation type, soil biogeochemical data, and upscaled soil carbon on South Baffin Island, Nunavut, Canada, 2022*. Arctic Data Center. https://doi.org/10.18739/A29Z90D69

Harden, J. W., Koven, C. D., Ping, C.-L., Hugelius, G., McGuire, A. D., Camill, P., et al. (2012). Field information links permafrost carbon to physical vulnerabilities of thawing. *Geophysical Research Letters*, *39*(15). https://doi.org/10.1029/2012GL051958

Henkner, J., Scholten, T., & Kühn, P. (2016). Soil organic carbon stocks in permafrost-affected soils in West Greenland. *Geoderma*, *282*, 147–159. https://doi.org/10.1016/j.geoderma.2016.06.021

Hicks Pries, C. E., Schuur, E. A. G., Vogel, J. G., & Natali, S. M. (2013). Moisture drives surface decomposition in thawing tundra. *Journal of Geophysical Research: Biogeosciences*, *118*(3), 1133–1143. https://doi.org/10.1002/jgrg.20089

Hobbie, S. E., Schimel, J. P., Trumbore, S. E., & Randerson, J. R. (2000). Controls over carbon storage and turnover in high-latitude soils. *Global Change Biology*, *6*(S1), 196–210. https://doi.org/10.1046/j.1365-2486.2000.06021.x

Horwath Burnham, J., & Sletten, R. S. (2010). Spatial distribution of soil organic carbon in northwest Greenland and underestimates of high Arctic carbon stores. *Global Biogeochemical Cycles*, *24*(3), GB3012. https://doi.org/10.1029/2009GB003660

Hossain, M. F., Chen, W., & Zhang, Y. (2015). Bulk density of mineral and organic soils in the Canada's Arctic and sub-Arctic. *Information Processing in Agriculture*, *2*(3–4), 3–4. https://doi.org/10.1016/j.inpa.2015.09.001

Hugelius, G. (2012). Spatial upscaling using thematic maps: An analysis of uncertainties in permafrost soil carbon estimates. *Global Biogeochemical Cycles*, *26*(2), GB2026. https://doi.org/10.1029/2011GB004154

Hugelius, G., Bockheim, J. G., Camill, P., Elberling, B., Grosse, G., Harden, J. W., et al. (2013). A new data set for estimating organic carbon storage to 3 m depth in soils of the northern circumpolar permafrost region. *Earth System Science Data*, *5*(2), 393–402. https://doi.org/10.5194/essd-5-393-2013

Hugelius, G., Kuhry, P., Tarnocai, C., & Virtanen, T. (2010). Soil organic carbon pools in a periglacial landscape: A case study from the central Canadian Arctic. *Permafrost and Periglacial Processes*, *21*(1), 16–29. https://doi.org/10.1002/ppp.677

Hugelius, G., Strauss, J., Zubrzycki, S., Harden, H. W., Schuur, E. A. G., Ping, C.-L., et al. (2014). Estimated stocks of circumpolar permafrost carbon with quantified uncertainty ranges and identified data gaps. *Biogeosciences*, *11*(23), 6573–6593. https://doi.org/10.5194/bg-11-6573-2014

Hugelius, G., Virtanen, T., Kaverin, D., Pastukhov, A., Rivkin, F. M., Marchenko, S., et al. (2011). High-resolution mapping of ecosystem carbon storage and potential effects of permafrost thaw in periglacial terrain, European Russian Arctic. *Journal of Geophysical Research*, *116*(G3), G03024. https://doi.org/10.1029/2010JG001606

Hung, J. K. Y., Scott, N. A., & Treitz, P. M. (2023). Drivers of soil nitrogen availability and carbon exchange processes in a High Arctic wetland. *Arctic Science*, *10*(1), 22–33. https://doi.org/10.1139/as-2022-0048

Jia, G. J., Epstein, H. E., & Walker, D. A. (2009). Vegetation greening in the Canadian Arctic related to decadal warming. *Journal of Environmental Monitoring*, *11*(12), 2231–2238. https://doi.org/10.1039/B911677J

Johnson, K. D., Harden, J., McGuire, A. D., Bliss, N. B., Bockheim, J. G., Clark, M., et al. (2011). Soil carbon distribution in Alaska in relation to soil-forming factors. *Geoderma*, *167–168*, 71–84. https://doi.org/10.1016/j.geoderma.2011.10.006

Juselius, T., Ravolainen, V., Zhang, H., Piilo, S. M., Gallego-Sala, A., Väliranta, M., & Väliranta, M. (2022). Newly initiated carbon stock, organic soil accumulation patterns and main driving factors in the High Arctic Svalbard, Norway. *Scientific Reports*, *12*(1), 4679. https://doi.org/10.1038/s41598-022-08652-9

Lamarque, L. J., Félix-Faure, J., Deschamps, L., Lévesque, E., Cusson, P.-O., Fortier, D., et al. (2023). Hydrological regime and plant functional traits jointly mediate the influence of Salix spp on soil organic carbon stocks in a High Arctic tundra. *Ecosystems*, *26*(6), 1238–1259. https://doi.org/10.1007/s10021-023-00829-1

Lara, M. J., McGuire, A. D., Euskirchen, E. S., Genet, H., Yi, S., Rutter, R., et al. (2020). Local-scale Arctic tundra heterogeneity affects regional-scale carbon dynamics. *Nature Communications*, *11*(1), 4925. https://doi.org/10.1038/s41467-020-18768-z

Loisel, J., Yu, Z., Beilman, D. W., Camill, P., Alm, J., Amesbury, M. J., et al. (2014). A database and synthesis of northern peatland soil properties and Holocene carbon and nitrogen accumulation. *The Holocene*, *24*(9), 1028–1042. https://doi.org/10.1177/0959683614538073

Lynch, L. M., Machmuller, M. B., Cotrufo, M. F., Paul, E. A., & Wallenstain, M. D. (2018). Tracking the fate of fresh carbon in the Arctic tundra: Will shrub expansion alter responses of soil organic matter to warming? *Soil Biology and Biochemistry*, *120*, 134–144. https://doi.org/10.1016/j.soilbio.2018.02.002

Maxwell, J. B. (1981). Climatic regions of the Canadian Arctic Islands. *Arctic*, *34*(3), 225–240. https://doi.org/10.14430/arctic2525

McFeeters, S. K. (1996). The use of the Normalized Difference Water Index (NDWI) in the delineation of open water features. *International Journal of Remote Sensing*, *17*(7), 1425–1432. https://doi.org/10.1080/01431169608948714

McGuire, A. D., Anderson, L. G., Christensen, T. R., Dallimore, S., Guo, L., Hayes, D. J., et al. (2009). Sensitivity of the carbon cycle in the Arctic to climate change. *Ecological Monographs*, *79*(4), 523–555. https://doi.org/10.1890/08-2025

Mekis, É., & Vincent, L. A. (2011). An overview of the second generation adjusted daily precipitation dataset for trend analysis in Canada. *Atmosphere-Ocean*, *49*(2), 163–177. https://doi.org/10.1080/07055900.2011.583910

Mekonnen, Z. A., Riley, W., Berner, L. T., Bouskill, N. J., Torn, M. S., Iwahana, G., et al. (2021). Arctic tundra shrubification: A review of mechanisms and impacts on ecosystem carbon balance. *Environmental Research Letters*, *16*(5), 053001. https://doi.org/10.1088/1748-9326/abf28b

Mekonnen, Z. A., Riley, W. J., Grant, R. F., Salmon, V. G., Iversen, C. M., Biraud, S. C., et al. (2021). Topographical controls on hillslope-scale hydrology drive shrub distributions on the Seward Peninsula, Alaska. *Journal of Geophysical Research: Biogeosciences*, *126*(2), e2020JG005823. https://doi.org/10.1029/2020JG005823

Metcalfe, D. B., Hermans, T. D. G., Ahlstrand, J., Becker, M., Berggren, M., Björk, R. G., et al. (2018). Patchy field sampling biases understanding of climate change impacts across the Arctic. *Nature Ecology & Evolution*, *2*(9), 1443–1448. https://doi.org/10.1038/s41559-018-0612-5

Michaelson, J., Ping, C. L., & Kimble, J. M. (1996). Carbon storage and distribution of tundra soils of Arctic Alaska, U.S.A. *Arctic and Alpine Research*, *28*(4), 414–424. https://doi.org/10.1080/00040851.1996.12003194

Mikola, J., Virtanen, T., Linkosalmi, M., Vähä, E., Nyman, J., Postanogova, O., et al. (2018). Spatial variation and linkages of soil and vegetation in the Siberian Arctic tundra—Coupling field observations with remote sensing data. *Biogeosciences*, *15*(9), 2781–2801. https://doi.org/10.5194/bg-15-2781-2018

Mishra, U., Hugelius, G., Shelef, E., Yang, Y., Strauss, J., Lupachev, A., et al. (2021). Spatial heterogeneity and environmental predictors of permafrost region soil organic carbon stocks. *Science Advances*, *7*(9), eaaz5236. https://doi.org/10.1126/sciadv.aaz5236

Mishra, U., Jastrow, J. D., Matamala, R., Hugelius, G., Coven, C. D., Harden, J. W., et al. (2013). Empirical estimates to reduce modeling uncertainties of soil organic carbon in permafrost regions: A review of recent progress and remaining challenges. *Environmental Research Letters*, *8*, 3. https://doi.org/10.1088/1748-9326/8/3/035020

Mishra, U., & Riley, W. J. (2012). Alaskan soil carbon stocks: Spatial variability and dependence on environmental factors. *Biogeosciences*, *9*, 3637–3645. https://doi.org/10.5194/bg-9-3637-2012

Nabe-Nielsen, J., Normand, S., Hui, F. K. C., Stewart, L., Bay, C., Nabe-Nielson, L. I., & Schmidt, N. M. (2017). Plant community composition and species richness in the High Arctic tundra: From the present to the future. *Ecology and Evolution*, *7*(23), 10233–10242. https://doi.org/10.1002/ece3.3496

Naito, A. T., & Cairns, D. M. (2011). Relationships between Arctic shrub dynamics and topographically derived hydrologic characteristics. *Environmental Research Letters*, *6*(4), 045506. https://doi.org/10.1088/1748-9326/6/4/045506

Natali, S. M., Schuur, E. A. G., Mauritz, M., Schade, J. D., Celis, G., Crummer, K. G., et al. (2015). Permafrost thaw and soil moisture driving CO_2 and CH_4 release from upland tundra. *Journal of Geophysical Research: Biogeosciences*, *120*(3), 525–537. https://doi.org/10.1002/2014JG002872

Neilson, B. T., Bayani Cardenas, M., O'Connor, M. T., Rasmussen, M. T., King, T. V., & Kling, G. W. (2018). Groundwater flow and exchange across the land surface explain carbon export patterns in continuous permafrost watersheds. *Geophysical Research Letters*, *45*(15), 7596–7605. https://doi.org/10.1029/2018GL078140

O'Conner, M. T., Bayani Cardenas, M., Ferencz, S. B., Wu, Y., Nielson, B. T., Chen, J., & Kling, G. W. (2020). Empirical models for predicting water and heat flow properties of permafrost soils. *Geophysical Research Letters*, *47*(11). https://doi.org/10.1029/2020GL087646

Osono, T., More, A. S., Uchida, M., & Kanda, H. (2016). Accumulation of carbon and nitrogen in vegetation and soils of deglaciated area in Ellesmere Island, high-Arctic Canada. *Polar Science*, *10*(3), 288–296. https://doi.org/10.1016/j.polar.2016.03.003

Ostendorf, B., & Reynolds, J. F. (1998). A model of arctic tundra vegetation derived from topographic gradients. *Landscape Ecology*, *13*(3), 187–201. https://doi.org/10.1023/A:1007986410048

Palmtag, J., Cable, S., Christiansen, H. H., Hugelius, G., & Kuhry, P. (2018). Landform partitioning and estimates of deep storage of soil organic matter in Zackenberg, Greenland. *The Cryosphere*, *12*(5), 1735–1744. https://doi.org/10.5194/tc-12-1735-2018

Palmtag, J., Hugelius, G., Laschinskiy, N., Tamstorf, M. P., Richter, A., Elberling, B., & Kuhry, P. (2015). Storage, landscape distribution, and burial history of soil organic matter in contrasting areas of continuous permafrost. *Arctic Antarctic and Alpine Research*, *47*(1), 71–88. https://doi.org/10.1657/AAAR0014-027

Palmtag, J., Ramage, J., Hugelius, G., Gentsch, N., Lashchinskiy, N., Richter, A., & Kuhry, P. (2016). Controls on the storage of organic carbon in permafrost soil in northern Siberia. *European Journal of Soil Science*, *67*(4), 478–491. https://doi.org/10.1111/ejss.12357

Petrenko, C. L., Bradley-Cook, J., Lacroix, E. M., Friedland, A. J., & Virginia, R. A. (2016). Comparison of carbon and nitrogen storage in mineral soils of graminoid and shrub tundra sites, western Greenland. *Arctic Science*, *2*(4), 165–182. https://doi.org/10.1139/as-2015-0023

Poggio, L., de Sousa, L. M., Batjes, N. H., Heuvelink, G. B. M., Kempen, B., Ribeiro, E., & Rossiter, D. (2021). SoilGrids 2.0: Producing soil information for the globe with quantified spatial uncertainty. *SOIL*, *7*(1), 217–240. https://doi.org/10.5194/soil-7-217-2021

Prowse, T. D., Furgal, C., Bonsal, B. R., & Peters, D. L. (2009). Climate impacts on Northern Canada: Regional background. *Royal Swedish Academy of Sciences*, *38*(5), 248–256. https://doi.org/10.1579/0044-7447-38.5.248

Räsänen, A., Juutinen, S., Tuittila, E.-S., Aurela, M., & Virtanen, T. (2019). Comparing ultra-high spatial resolution remote-sensing methods in mapping peatland vegetation. *Journal of Vegetation Science*, *30*(5), 1016–1026. https://doi.org/10.1111/jvs.12769

R Core Team. (2023). *R: A language and environment for statistical computing*. R Foundation for Statistical Computing. Retrieved from https://www.R-project.org/

Schuur, E., McGuire, A., Schädel, C., Grosse, G., Harden, J. W., Hayes, D. J., et al. (2015). Climate change and the permafrost carbon feedback. *Nature*, *520*(7546), 171–179. https://doi.org/10.1038/nature14338

Schuur, E., Vogel, J., Crummer, K., Lee, H., Sickman, J. O., & Osterkamp, T. E. (2009). The effect of permafrost thaw on old carbon release and net carbon exchange from tundra. *Nature*, *459*(7246), 556–559. https://doi.org/10.1038/nature08031

Siewert, M. B. (2018). High-resolution digital mapping of soil organic carbon in permafrost terrain using machine learning: A case study in a sub-Arctic peatland environment. *Biogeosciences*, *15*(6), 1663–1682. https://doi.org/10.5194/bg-15-1663-2018

Siewert, M. B., Hanisch, J., Weiss, N., Kuhry, P., Maximov, T. C., & Hugelius, G. (2015). Comparing carbon storage of Siberian tundra and taiga permafrost ecosystems at very high spatial resolution. *Journal of Geophysical Research: Biogeosciences*, *120*(10), 1973–1994. https://doi.org/10.1002/2015JG002999

Siewert, M. B., Hugelius, G., Heim, B., & Faucherre, S. (2016). Landscape controls and vertical variability of soil organic carbon storage in permafrost-affected soils of the Lena River Delta. *Catena*, *147*, 725–741. https://doi.org/10.1016/j.catena.2016.07.048

Stehman, S. V. (1997). Selecting and interpreting measures of thematic classification accuracy. *Remote Sensing of Environment*, *62*(1), 77–89. https://doi.org/10.1016/S0034-4257(97)00083-7

Sterner, R. W., & Elser, J. J. (2002). *Ecological stoichiometry: The biology of elements from molecules to the biosphere* (p. 464). Princeton University Press.

Tarnocai, C., Canadell, J. G., Schuur, E. A. G., Kuhry, P., Mazhitova, G., & Zimov, S. (2009). Soil organic pools in the northern circumpolar permafrost region. *Global Biogeochemical Cycles*, *23*(2), GB2023. https://doi.org/10.1029/2008GB003327

Turetsky, M. R., Abbott, B. W., Jones, M. C., Anthony, K. W., Olefeldt, D., Schuur, E. A. G., et al. (2020). Carbon release through abrupt permafrost thaw. *Nature Geoscience*, *13*(2), 138–143. https://doi.org/10.1038/s41561-019-0526-0

Virkkala, A.-M., Abdi, A. M., Luoto, M., & Metcalfe, D. B. (2019). Identifying multidisciplinary research gaps across Arctic terrestrial gradients. *Environmental Research Letters*, *14*(12), 124061. https://doi.org/10.1088/1748-9326/ab4291

Walker, D. A., Raynolds, M. K., Daniëls, F. J. A., Einarsson, E., Elvebakk, A., Gould, W. A., et al. (2005). The circumpolar Arctic vegetation map. *Journal of Vegetation Science*, *16*(3), 267–282. https://doi.org/10.1111/j.1654-1103.2005.tb02365.x

Weintraub, M., & Schimel, J. (2003). Interactions between carbon and nitrogen mineralization and soil organic matter chemistry in Arctic tundra soils. *Ecosystems*, *6*(2), 0129–0143. https://doi.org/10.1007/s10021-002-0124-6

Weiss, N., Faucherre, S., Lampiris, N., & Wojcik, R. (2017). Elevation-based upscaling of organic carbon stocks in High-Arctic permafrost terrain: A storage and distribution assessment for Spitsbergen, Svalbard. *Polar Research*, *36*(1), 1400363. https://doi.org/10.1080/17518369.2017.1400363

Wojcik, R., Palmtag, J., Hugelius, G., Weiss, N., & Kuhry, P. (2019). Land cover and landform-based upscaling of soil organic carbon stocks on the Brøgger Peninsula, Svalbard. *Arctic Antarctic and Alpine Research*, *51*(1), 40–57. https://doi.org/10.1080/15230430.2019.1570784

Yang, D., Morrison, B. D., Hantson, W., Breen, A. L., McMahon, A., Li, Q., et al. (2021). Landscape-scale characterization of Arctic tundra vegetation composition, structure, and function with a multi-sensor unoccupied aerial system. *Environmental Research Letters*, *16*(8), 085005. https://doi.org/10.1088/1748-9326/ac1291

Yonghong, Y., Bakian-Dogaheh, K., Moghaddam, M., Mishra, U., & Kimball, J. S. (2023). Mapping surface organic soil properties in Arctic tundra using C-Band SAR Data. *Ieee Journal of Selected Topics in Applied Earth Observations and Remote Sensing*, *16*, 1403–1413. https://doi.org/10.1109/JSTARS.2023.3236117

Zoltai, S. C. (1978). A portable sampler for perennially frozen stone-free soils. *Canadian Journal of Soil Science*, *58*(4), 521–523. https://doi.org/10.4141/cjss78-058